

4-Hydroxy-benzoic acid (4-diethylamino-2-hydroxy-benzylidene)hydrazide: DFT, antioxidant, spectroscopic and molecular docking studies with BSA

Vibha Sharma,* Ekta Kundra Arora and Savio Cardoza

ABSTRACT: The Schiff base 4-hydroxy-benzoic acid (4-diethylamino-2-hydroxy-benzylidene) hydrazide (SL) was synthesized and characterized. Its antioxidant activity was evaluated using 1,1-diphenyl-2-picrylhydrazyl (DPPH) free radical scavenging action. Being a potent antioxidant its binding ability to the transport protein bovine serum albumin (BSA) was studied using fluorescence quenching and circular dichroism (CD) studies. The binding distance has been calculated by fluorescence resonance energy transfer (FRET) to be 1.85 Å and the Stern–Volmer quenching constant has been calculated to be $(3.23 \pm 0.45) \times 10^5 \text{ M}^{-1}$. Quantum chemical analysis was carried out for the Schiff base using DFT with B3LYP and 6–311G** and related to the experimentally obtained results. For a deeper understanding of the mechanism of the interaction, the experimental data were complemented by protein–Schiff base docking calculations using Argus Lab. Copyright © 2015 John Wiley & Sons, Ltd.

Additional supporting information may be found in the online version of this article at the publisher's web site.

Keywords: Schiff base; antioxidant activity; quantum chemical analysis; protein–Schiff base docking studies

Introduction

Numerous compounds of biological interest both natural and man-made have the Schiff base nucleus. These compounds show potent antioxidant, antibacterial, antiviral, analgesic, antiplatelet, antimicrobial, antimalarial and anticancer activities as revealed by literature studies (1–4). The azomethine linkage in these compounds is of prime importance as it is instrumental in these compounds exhibiting antitumor activity (5). Serum albumin is the most abundant plasma protein in mammals. It acts as a transport protein for a wide variety of drugs, nutrients, metabolites and molecules of diverse nature. It is a single chain protein which is also responsible for the maintenance of blood pH. The pharmaceutical, biochemical applications stem from its ligand binding ability. It is one of the most widely studied proteins (6). Bovine serum albumin (BSA) is usually used as a protein concentration standard in lab experiments. BSA has two tryptophan residues, which significantly contribute to the intrinsic fluorescence of this protein (7). It has remarkably high affinity for a variety of ligands. Extensive experiments with the aim of characterizing the binding capacity and binding sites of albumins have been carried out. The serum albumins also show remarkable sequence and structural similarity (8). The spectral changes observed on the binding of fluorophores with proteins are important tools for the investigations of, the topology of the binding sites, the conformational changes and for the characterization of substrate to ligand binding. Serum albumins which are the major transport proteins for the drugs and other physiological substances are considered as a model for studying these drug–protein interaction (9,10). An understanding of how the chemical structure relates to the chemical and the biological activity of compounds can be obtained by quantum chemical analysis (11–14). This aids in understanding and development

of new potent therapeutic agents. The target of the present investigation is to synthesize and evaluate the electronic and molecular properties of the Schiff base, SL, to investigate its antioxidant potential and study its binding ability to BSA using a fluorescence quenching technique, CD studies and molecular docking. Molecular docking allows us to understand the ligand–protein interactions. The docking analysis of BSA with SL was carried out by Argus Lab Docking software. The electronic and molecular properties have been calculated using the DFT with B3LYP and the possible places of electrophilic attack and hydrogen bond formation have been predicted. Antioxidants are needed to protect the cell from oxidative damage that can be induced by free radicals. The antioxidant donates the hydrogen to the free radical and itself gets reduced to a harmless unreactive form (15). Schiff bases are known to be potent antioxidants sometimes even better than ascorbic acid.

Experimental

All chemicals and BSA were purchased from Sigma (A.R. Grade) and used as such without further purification. The BSA solution

* Correspondence to: Vibha Sharma, Chemistry Department, St. Stephen's College, University of Delhi, Delhi 110007, India.
E-mail: vibhasharmastephens@hotmail.com

Chemistry Department, St. Stephen's College, University of Delhi, Delhi 110007, India

Abbreviations:: BSA, bovine serum albumin; CD, circular dichroism; DFT, density functional theory; DPPH, 1,1-diphenyl-2-picrylhydrazyl; FRET, fluorescence resonance energy transfer.

was prepared in the phosphate buffer pH 7.4 and kept in the dark. The work was carried out using double distilled water. Antioxidant activity was measured using DPPH free radical assay. A Varian spectrofluorometer, with a 150 W xenon lamp was used to measure the fluorescence. The fluorescence quenching of BSA was recorded in the wavelength range 290–500 nm after exciting the protein at 280 nm, using 5 nm/5 nm as slit widths with increasing Schiff base concentration. ¹H-NMR spectra have been recorded using JNM-EXCP, a 400 MHz instrument. The UV–visible spectra have been measured using the UV-visible spectrophotometer (Specord 250). Mass spectra have been recorded using Agilent Technologies 6530 accurate mass Q-TOF LC/MS. The CD has been recorded on the Jasco circular dichroism spectropolarimeter model J-810. CHN analysis was performed on Elementar analysensysteme Germany, model Vario-micro cube. Spectroscopic grade solvents were used throughout. Melting points were measured on a Digital Melting point apparatus (PL Scientific Instruments) and are uncorrected.

Synthesis of Schiff base SL

One equivalent of 4-(diethylamino)-salicylaldehyde was dissolved in ethanol and 1 equivalent of 4-hydroxybenzohydrazide was dissolved in minimum amount of 1 N HCl. The solution of 4-hydroxybenzohydrazide was added drop-wise to the hot solution of 4-(diethylamino)-salicylaldehyde with continuous stirring. The reaction was refluxed for 3 h and the reaction mixture added to crushed ice. The precipitate formed was filtered and washed with dilute HCl and water. The crude product was recrystallized with ethanol. Yield 60%; colour: pale green, M.P.: 220–222°C.

Antioxidant studies

The antioxidant activity of SL was measured using DPPH radicals as the hydrogen acceptors by Blois method (16). 0.5 mL of 0.5, 0.25, 0.125, and 0.156 mmol of SL was mixed with 0.3 mL of 1 mM DPPH dissolved in ethanol and the total volume was made up to 3.8 mL using ethanol. The reaction mixture was incubated in the dark for 100 min at 28°C. The control contained a mixture of 3.5 ml ethanol and 0.3 ml DPPH solution whereas the blank was a mixture of 3.3 ml ethanol and 0.5 mL sample solution. The DPPH radical scavenging activity was determined by measuring the absorbance at 517 nm using the UV-visible spectrophotometer. The scavenging activity was calculated using equation (1) where A_{blank} is the absorbance of the blank solutions, A_{sample} is the absorbance in the presence of the samples or standards and A_{control} is the absorbance of the control:

$$\text{Scavenging Effect\%} = 100 - \frac{[(A_{\text{sample}} - A_{\text{blank}}) \times 100]}{A_{\text{control}}} \quad (1)$$

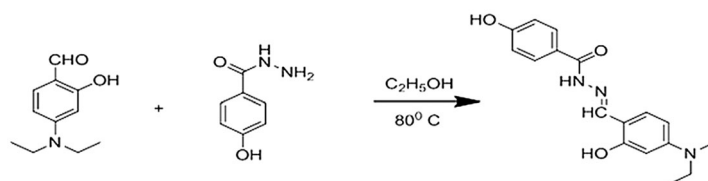


Figure 1. Synthesis of Schiff base SL.

Protein binding studies

The UV–visible absorption spectra of BSA were recorded with increasing concentration of the Schiff base SL in the wavelength range 200 to 320 nm. For fluorescence measurements all samples were prepared in 0.1 M phosphate buffer (pH = 7.4). The fluorescence quenching of BSA was recorded with increasing concentrations of SL after exciting the protein solution at 280 nm, with 5 nm/5 nm slit widths. The protein concentration was fixed at 3×10^{-6} M and the concentration of SL was varied from 0–5 times that of the protein. The inner filter effect in the case of pH-dependent titrations was negligible and therefore no corrections were applied.

Computational studies

All theoretical studies were performed with the Turbomole program package. The electronic and molecular properties have been calculated using DFT with B3LYP using the basis set 6–311G**.

Docking studies

The crystal structure of BSA (PDB Id:4OR0) (17) was downloaded from the Brookhaven Protein Data Bank. The non-essential water molecules were removed and protein structure prepared for docking. The 3-D structure of SL was generated and optimized by Turbomole software. Molecular docking studies on BSA-SL binding were performed with Arguslab 4.0.1 software (18). The docking runs with a maximum of 200 candidate poses were performed on the ArgusDock docking engine using high precision.

Results and discussion

The Schiff base SL was synthesized by the reaction between 4-(diethylamino)-salicylaldehyde and 4-hydroxybenzohydrazide (Fig. 1). CHN $C_{18}H_{21}N_3O_3$; C 66.04; H 6.47; N12.84 Found C 65.48; H 7.45; N 12.69. IR spectra (Fig. S1) (KBr pellet) $\nu(\text{cm}^{-1})$ 1628 (C=O stretching), 3345 (O–H stretching) 3226 (N–H stretching), 1017 (N–N stretching), 1597 (C=N) stretching. ¹H-NMR (Fig. S2) (CDCl_3 , δ ppm) 8.3 (s,1H,CH=N), 2.00 (s,4H,2CH₂), 1.15 (s,6H,2CH₃), 6.2–7.9 (m,7H,benzene rings) 10.1 (s,1H,NH), 11.3 (s,2H,2OH). UV/VIS (Fig. S3): 368 nm (π – π^*), 275 nm (n – π^*) transitions of the imine in ethanol. MS (Fig. S4): m/z (M^+) 327.15; ($M+H$)⁺328.16.

Antioxidant studies

The DPPH assay was performed. The results are given in Fig. 2 and Table S1. The dark-coloured DPPH radical solution turned to yellow-coloured diphenylpicrylhydrazine in the presence of the antioxidant compound and the absorbance of the solution decreases. A notable decline in the concentration of DPPH radical in terms of % inhibition was observed due to the scavenging

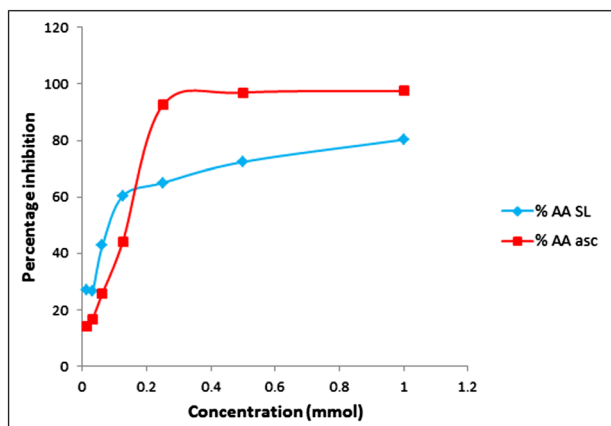


Figure 2. Plot of % inhibition of the DPPH versus concentration of SL and ascorbic acid (asc).

ability of SL. The inhibition percentage of the sample showed a concentration-dependent pattern (Fig. 2). The IC_{50} value was found out to be $69 \mu\text{g/mL}$ indicating that it is a potent antioxidant. The value obtained for ascorbic acid is $38 \mu\text{g/mL}$.

Protein binding studies (fluorescence quenching)

The wavelength of maximum absorbance for SL and BSA in the phosphate buffer medium is 368 and 281 nm. As the concentration of SL increases the intensity of absorbance of BSA decreases and the peak at 210 nm is red shifted. In addition, the absorption peaks in the UV-visible spectra at approximately 280 nm rise gradually and are blue shifted by about 5 nm with increasing concentration of the Schiff base. These results indicate the interaction between the Schiff base and BSA, the fluorescence quenching of BSA occurring as a result of complex formation (Fig. 3). The changes in the tertiary structure of BSA were analysed by fluorescence spectroscopy in the presence of different concentrations of SL in 0.1 M phosphate buffer (pH = 7.4). The fluorescence spectra of BSA ($3 \times 10^{-6} \text{ M}$) with increasing concentrations of the Schiff base (0–5 times the protein) were recorded in the range of 290–500 nm. The emission maximum shifts from 344 to 337 nm and a decrease in fluorescence is observed as the Schiff base

concentration increases. This implies that binding of the Schiff base to the protein results in change in solvent accessibility of the protein (19). The variation in fluorescence intensity is presented in the Fig. 4(a, b).

The Stern–Volmer equation (equation (2)) has been used to analyse the data obtained from the fluorescence study of the quenching process. The F_0 and F are the steady state fluorescence intensities at the maximum wavelength in the absence and presence of quencher, respectively, $[Q]$ is the quencher concentration and K_{SV} is the Stern–Volmer constant (20):

$$\frac{F}{F_0} = 1 + K_{sv}[Q] \quad (2)$$

The Stern–Volmer plot shows upward curvature suggesting a complex quenching process which may be both static and dynamic in nature (Fig. 5a) (21,22).

The bimolecular quenching rate constant K_q was evaluated using equation (3) where τ_0 is the average lifetime of the protein without the quencher:

$$K_q = K_{sv}/\tau_0 \quad (3)$$

The average fluorescence lifetime used was 10^{-8} (23). The K_{SV} is found out to be $(3.23 \pm 0.45) \times 10^5 \text{ M}^{-1}$ and the bimolecular quenching constant $3.23 \times 10^{13} \text{ L M}^{-1} \text{ s}^{-1}$. This is greater than the maximum scatter collision quenching constant of the biomolecule (24) ($K_q = 2.0 \times 10^{10} \text{ L M}^{-1} \text{ s}^{-1}$). The quenching is therefore mainly static in nature.

When the Schiff base molecules bind independently to a set of equivalent sites on a macromolecule, the equilibrium between free and bound molecules is given by equation (4):

$$\log[(F_0 - F)/F] = n \times \log K - n \times \log \frac{1}{[L_t] \frac{(F_0 - F)}{F_0} \times [P_t]} \quad (4)$$

where K is the binding constant, n is the number of binding sites and L_t and P_t are the total ligand and protein concentrations respectively. The values of K and n are 6.63×10^5 and 1.3 ± 0.15 at 25°C .

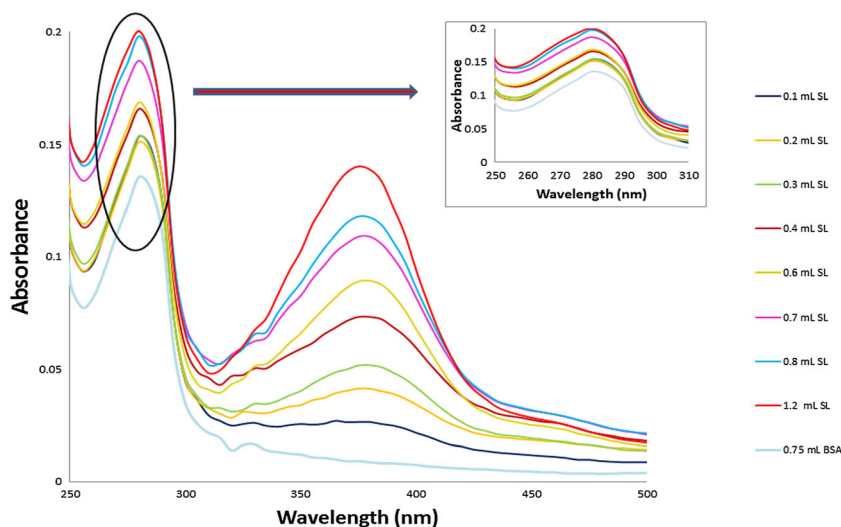


Figure 3. UV/VIS spectra of BSA at different concentrations SL.

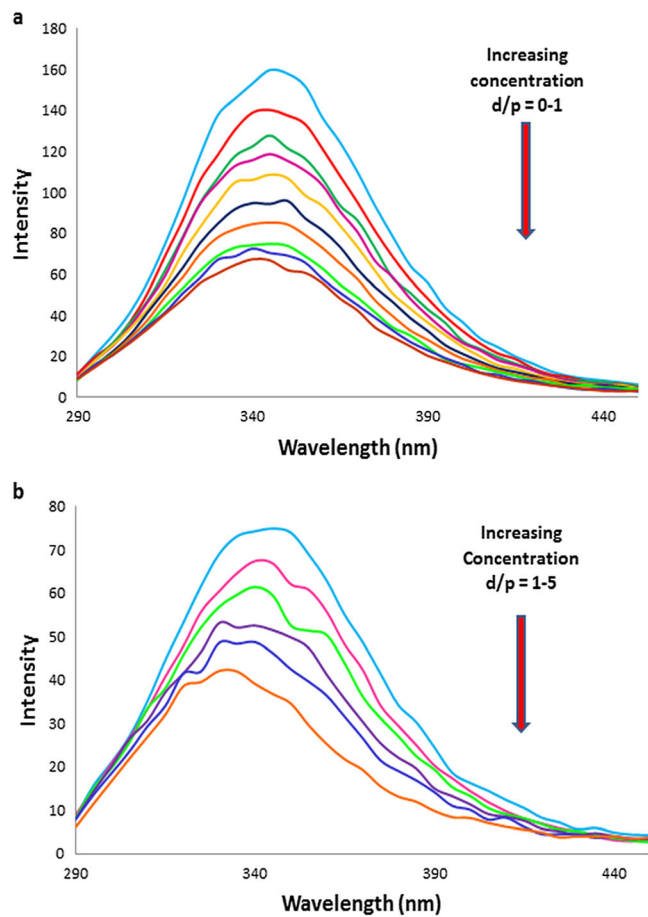


Figure 4. Emission spectra of BSA in the presence of different concentrations of SL: [BSA] = 3×10^{-6} M; (a) $d/p = 0-1$ (b) $d/p = 1-5$; $\lambda_{\text{exc}} = 286$ nm; pH = 7.4.

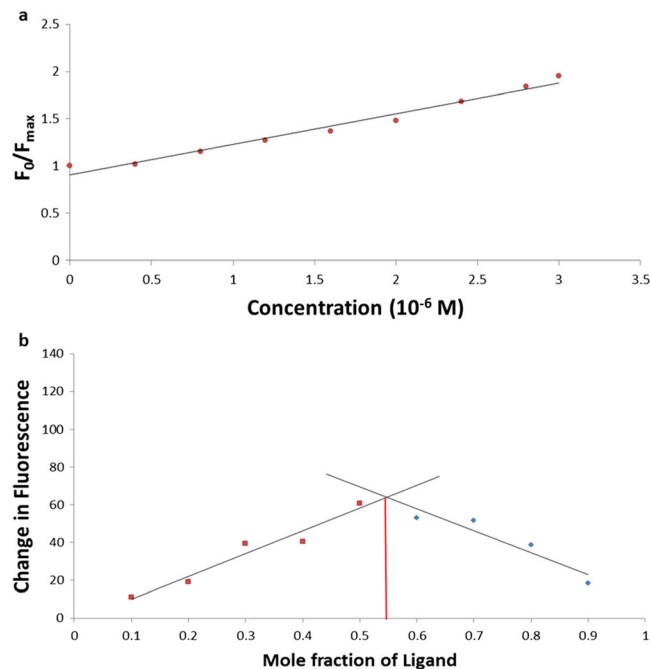


Figure 5. (a) Stern–Volmer plot of F_0/F_{max} against [Schiff base]; and (b) Job's method of continuous variations plot for BSA and SL.

The free energy change for the interaction between SL and BSA was evaluated using equation (5), where K and R are the binding constant and gas constant, respectively:

$$\Delta G = -RT \ln K \quad (5)$$

The ΔG value is found out to be -33.22 kJ M^{-1}

The stoichiometry of BSA and SL binding was determined by the method of continuous variation (25). The fluorescence measurements of a series of BSA–SL mixtures were done, where the mol fraction of the components was varied while the molarity of the mixture was a constant. The Job's plot is presented in Fig. 5(b). It shows that SL interacts with BSA in the ratio 1:1.

Fluorescence resonance energy transfer (FRET)

The absorption spectrum of SL (3×10^{-6} M) and the emission spectrum of BSA (3×10^{-6} M at excitation wavelength 280 nm) were recorded in the range of 300–500 nm. The overlap of the UV absorption spectrum of SL with the fluorescence emission spectrum of protein was used to calculate the energy transfer as per the Forster's theory (26) (Fig. 6). The molecular distance r between the protein and the Schiff base can be determined by FRET.

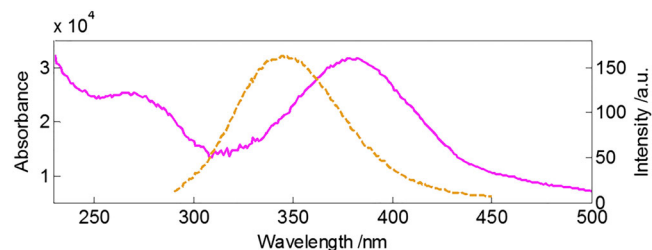


Figure 6. The overlap of the fluorescence spectrum of BSA and the absorption spectrum of the Schiff base SL.

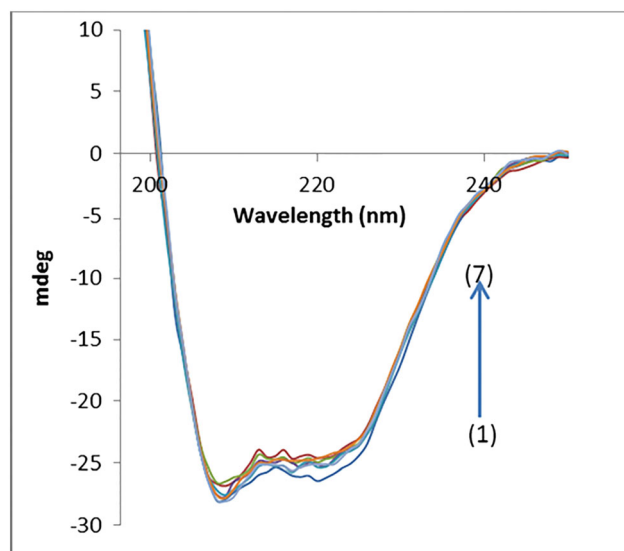


Figure 7. CD spectra of BSA with increasing amounts of SL.

According to Forster's non-radiative energy transfer theory, the energy transfer efficiency (E) can be defined by the following equations (6–8).

$$E = 1 - (F/F_0) = R_0^6 / (R_0^6 + r_0^6) \quad (6)$$

$$R_0^6 = 8.8 \times 10^{-25} [k^2 n^{-4} \phi_D J(\lambda)] \text{ in } \text{Å} \quad (7)$$

$$J(\lambda) = \int F_D(\lambda) \epsilon_A(\lambda) \lambda^4 d\lambda \quad (8)$$

where E is the efficiency of transfer between the donor and the acceptor, R_0 is the critical distance when the efficiency of transfer is 50%. $F_D(\lambda)$ is the corrected fluorescence intensity of the donor at wavelength λ to $(\lambda + d\lambda)$, with the total intensity normalized to unity and $\epsilon_A(\lambda)$ is the molar extinction coefficient of the acceptor

Table 1. Alteration in the secondary structure of the protein by interaction with SL

S. No.	d/p	α -Helix (%)	β -Sheet (%)
1	#	67.38	8.61
2	0.26	65.95	8.78
3	0.80	65.94	8.79
4	1.00	66.71	8.77
5	1.33	66.89	8.68
6	2.66	66.34	8.79
7	4.27	66.87	8.78

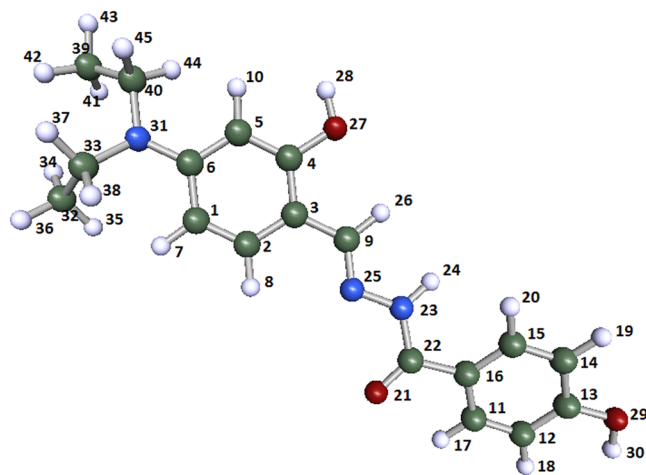


Figure 8. Geometry optimized structure of SL obtained using the DFT-B3LYP/6-311G**level of theory.

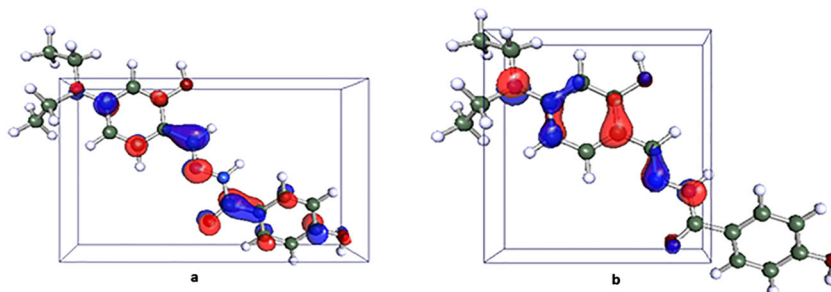


Figure 9. (a) The HOMO (b) The LUMO of the molecule SL.

at wavelength λ . J is the overlap integral of the fluorescence emission spectrum of the donor and the absorption spectrum of the acceptor. The value of k^2 , n and ϕ_D for BSA are 2/3, 1.336 and 0.118 (27). The calculated parameters are $J = 3.79 \times 10^{-22} \text{ cm}^3 \text{ L mol}^{-1}$, $R_0 = 1.88 \text{ Å}$, $E = 0.54$ and $r = 1.85 \text{ Å}$. The Forster's distance R_0 and the distance between the compound studied and the tryptophan residue r , were found to be 1.88 and 1.85 Å respectively. The maximal critical distance range for R_0 is from 5 to 10 nm and the maximum distance between donor and acceptor, r is in the range of 7–10 nm (25). These values of R_0 and r suggest that non-radiative transfer occurred between the Schiff base and BSA.

Circular dichroism (CD) analysis

CD measurements of BSA ($3 \times 10^{-6} \text{ M}$) in the presence and absence of SL were made using a quartz cell of 0.1 cm. The spectra were recorded at 25°C and the temperature was maintained constant by a thermostatically controlled circulating water bath. BSA to SL concentrations of d/p values 0, 0.26, 0.80, 1.00, 1.33, 2.66 and 4.26 were used for CD measurements.

CD spectroscopy is a sensitive tool to analyse changes in the secondary structure of the protein on ligand binding. The CD spectra of BSA in the absence and presence of SL was recorded (Fig. 7). The α -helix and β sheet contents of the free and combined BSA were calculated (Table 1). The K2D3 web server has been used to estimate the α helix and β sheet content of the protein from its CD spectrum (28). BSA shows negative bands in the ultraviolet region at 208 and 222 nm, characteristic for the α -helical structure (29–34). The results show that some conformational changes to α helix does occurs due to addition of SL but the structure overall retains its α -helix form.

Computational studies

The geometry optimization of the compound was carried out at DFT level using B3LYP functional and 6–311G** basis sets for all atoms without any symmetry restrictions. Population analysis based on occupation numbers (PABOON) were used as implemented in PABOON. The theoretically obtained geometry optimized structure of the molecule is shown in Fig. 8. The geometry optimized parameters of SL are given in Table S2. The thermochemical data for the hydrazone SL calculated at 298.15 K and 0.1 MPa pressure are provided in Table S3.

The Frontier Molecular Orbitals (HOMO and LUMO) and the ionization potential play an important role in determining the optical and electric properties and molecular reactivity of the compound. The single point energy, the energy of the HOMO and LUMO and the ionization potential were calculated according to the quantum chemical calculations. The energies of the HOMO and LUMO have

Table 2. PABOON analysis of SL obtained using the DFT-B3LYP/6-311G**level of theory

Atom	Charge	Atom	Charge	Atom	Charge
1c	-0.1297	16c	-0.134	31n	-0.0825
2c	0.0468	17h	0.0473	32c	-0.1488
3c	-0.0972	18h	0.0289	33c	-0.0275
4c	0.2362	19h	0.0358	34h	0.0458
5c	-0.2135	20h	0.0259	35h	0.0497
6c	0.1525	21o	-0.4076	36h	0.0402
7h	0.0323	22c	0.3865	37h	0.0469
8h	0.0464	23n	-0.0769	38h	0.0547
9c	0.0613	24h	0.0899	39c	-0.1556
10h	0.0235	25n	-0.1037	40c	0.0005
11c	0.0365	26h	0.0013	41h	0.0505
12c	-0.1198	27o	-0.2166	42h	0.0449
13c	0.197	28h	0.1407	43h	0.045
14c	-0.0551	29o	-0.1995	44h	0.0447
15c	-0.0173	30h	0.1431	45h	0.0307

been calculated to be -5.02 eV and -1.22 eV. The HOMO–LUMO gap is 3.891 eV and the dipole moment of the molecule is 4.917 Debye.

The HOMO can act as an electron donor, and the LUMO can act as an electron acceptor (35). As seen in Fig. 9(a, b), the HOMO is centered about the salicylaldehyde benzene ring, the phenolic oxygen, azomethine linkage and imine nitrogen while LUMO is centered about the 4-hydroxybenzhydrazide ring, the carbonyl carbon atom with some contributions from other atoms. In fact, the HOMO though not a direct descriptor can be related to electron transfer reactions and is very important in determining the antioxidant activity. A low value of HOMO energy can be correlated to a low electron-donating ability while a high value of HOMO energy correlates with good electron-donor ability to empty orbitals of suitable energy in an acceptor (36). Ascorbic acid with which the antioxidant behavior of SL has been compared experimentally has a HOMO value of -6.80 eV. The ionization potential (IP) which is also an indication of the nucleophilicity of the compound is the energy required for the abstraction of an electron in the molecule, which is the first step in the antioxidant mechanism. Many authors have related the IP to antioxidant activity. Molecules with low IP values can undergo oxidation easily. The adiabatic IP was calculated as the energy difference between the neutral molecule and its respective cation free radical. The value for the compound SL is found out to be 6.13 eV. These values of HOMO and IP will be useful when comparing with other potential antioxidant molecules. Theoretical UV/Vis spectra of SL

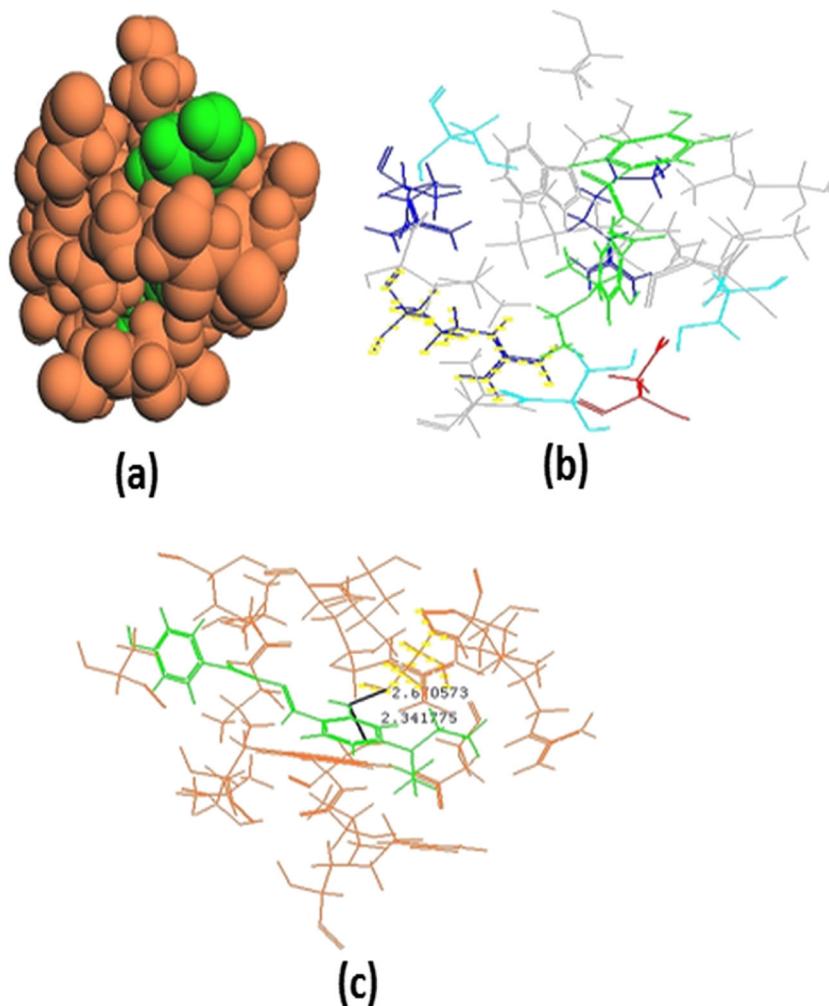


Figure 10. Computational model of SL docked into BSA in subdomain IIA. (a) SL (green) in BSA cavity (red). (b) Amino acids surrounding the Schiff base as shown by their polarity, red: Asp; dark blue: Arg; light blue: Ser. The other hydrophobic amino acids are grey. (c) Hydrogen bonds between the Schiff base and the amino acids in the protein.

obtained using the DFT-B3LYP/6-311G** level of theory is given in Fig. S5.

Phenolic hydroxyl groups are good hydrogen donors: hydrogen-donating antioxidants can react with reactive oxygen and reactive nitrogen which stops the cyclic process of generation of radicals (37,38). This results in the radical form of the antioxidant, stabilized by delocalization of the electron with the benzene ring. The antioxidant capacity of phenolic compounds and all compounds in general is also attributed to their ability to chelate metal ions involved in the production of free radicals (39). Based on the optimized structure of the title compound, the PABOON analysis (Table 2) was carried out to examine the relationship between the electrochemical properties and molecular structures of potential antioxidants (40). A high electron density is located at the carbonyl oxygen O₂₁ and the oxygen atom of the phenolic group O₂₇. This is followed by the nitrogen atom N₂₅. This finding implies that these atom groups are potential nucleophilic sites and can play an important role in the antioxidant activity of the compound by chelation or hydrogen abstraction. In fact the most nucleophilic positions of O₂₁ and O₂₇ contribute to the HOMO.

Docking studies

Argus Lab 4.0.1 was used to dock the Schiff base and determine its binding site in the protein. Crystalline BSA has three homologous domains (I, II, and III): each of these domains has two subdomains (A and B), which are divided into nine loops by 17 disulphide bonds, each one formed by six helices and its secondary structure is dominated by an α -helix (41,42). The principal regions of Schiff base binding to BSA are located in hydrophobic cavities in subdomains IIA and IIIA, and one tryptophan residue (Trp-212) of BSA is in subdomain IIA (43). The domains II and III share a common interface, binding of a probe to domain III leads to conformational changes affecting the binding affinities to domain II and vice versa (43). The docking results reveal that SL is located within the subdomain IIA whereas Try 213 is located in a hydrophobic cavity that is in close proximity to positively charge hydrophobic residues, such as Ala 209, Val 342, 481, Leu 197, 346, 454, 480, Trp 213 as seen in Fig. 10.

This suggests a hydrophobic interaction between the protein and the Schiff base. It also explains the efficient fluorescence quenching of BSA emission in the presence of SL. A number of specific electrostatic interactions and hydrogen bond interactions exist and play an important role in stabilizing the molecule. The formation of hydrogen bonds decreased the hydrophilicity and increases the hydrophobicity which helps stabilizing SL-BSA system. Hydrogen bonding interactions exist between the C=O of the Schiff base and OH of Ser 343 and Ser 453. The hydrogen bond distance between the carbonyl carbon and serine 343 being 2.34 Å and the carbonyl group and Ser 453 being 2.67 Å. Figure 10 shows SL surrounded by the amino acids (coloured with respect to the polarity) red: Asp; dark blue: Arg; light blue: Ser. The other hydrophobic amino acids are grey. Our fluorescence studies show a blue shift on complex formation which also supports the hydrophobic association.

Conclusion

The antioxidant properties of SL have been evaluated experimentally and by quantum chemical analysis. The interaction of this potent antioxidant SL with BSA has been investigated at pH 7.4, the physiological pH using different optical (fluorescence quenching

technique and CD) and computational techniques. The results show that SL binds to the BSA molecules and efficiently quenches its intrinsic fluorescence by static mechanism. The UV-visible studies also corroborated that the interaction between SL and BSA in the ratio 1:1. The molecular docking studies indicate a hydrophobic interaction between the protein and the Schiff base in a binding pocket near Try 213. These studies have helped in establishing the chemico-biological interactions of a potential therapeutic compound which will further aid in drug designing.

Acknowledgements

The authors are grateful the University Grants Commission (UGC) for financial support. One of the authors (SC) is thankful to the UGC for grant of Project Fellowship under Major Research Project scheme (F. No. 42-380/2013(SR)).

References

1. Sathe BS, Jaychandran E, Jagtap VA, Sreenivasa GM. Synthesis characterization and anti-inflammatory evaluation of new fluorobenzothiazole Schiff's bases. *Int J Pharm Res Dev* 2011;3:164-9.
2. Sakiyan I, Loğoğlu E, Arslan S, Sari N, Sakiyan N. Antimicrobial activities of N-(2-hydroxy-1-naphthalidene)-aminoacid (glycine, alanine, phenylalanine, histidine, tryptophane) Schiff bases and their manganese(III) complexes. *BioMetals* 2014;17:115-20.
3. Varandas LS, Fraga CAM, Miranda ALP, Barreiro EJ. Design, synthesis and pharmacological evaluation of new nonsteroidal antiinflammatory 1,3,4-thiadiazole derivatives. *Lett Drug Des Discov* 2005;2:62-65.
4. Swathi K, Sarangapani M. Synthesis and anti-inflammatory activity of a novel series of Isatin hydrazone and Isatin thiosemicarbazone derivatives. *World J Pharmacy Pharm Sci* 2014;3:2070-78.
5. Rollas S, Guniz Kucukguzel S. Biological activities of hydrazone derivatives. *Molecules* 2007;12:1910-39.
6. Figge J, Rossing TH, Fencel V. The role of serum proteins in acid-base equilibria. *J Lab Clin Med* 1991;117:453-67.
7. Trnková L, Boušová I, Kubiček V, Dršata J. Binding of naturally occurring hydrocinamic acids to Bovine Serum Albumin. *Nat Sci* 2010;2:563-570.
8. Bujacz A, Zielinski K, Sekula B. Structural studies of bovine, equine and leporine serum albumin complexes with naproxen. *J Proteins* 2014;82:2199-208.
9. Valentão P, Fernandes E, Carvalho F, Andrade PB, Seabra RM, Bastos ML. Hydroxyl radical and hypochlorous acid scavenging activity of small centaury (*Centaureum erythraea*) infusion. A comparative study with green tea (*Camellia sinensis*). *Phytomedicine* 2003;10:517-22.
10. Trnková L, Boušová I, Kubiček V, Dršata J. Binding of naturally occurring hydroxycinnamic acids to bovine serum albumin. *J Nat Sci* 2010;2:563-70.
11. Heim KE, Tagliaferro AR, Bobilya DJ. Flavonoid antioxidants: chemistry, metabolism and structure-activity relationships. *J Nutrit Biochem* 2002;13:572-84.
12. Payá M, Halliwell B, Hoult JRS. Interactions of a series of coumarins with reactive oxygen species. Scavenging of superoxide, hypochlorous acid and hydroxyl radicals. *Biochem Pharmacol* 1992;44:205-14.
13. Choi HR, Choi JS, Han YN, Bae SJ, Chung HY. Peroxynitrite scavenging activity of herb extracts. *Phytother Res* 2002;16:364-7.
14. Yang CS, Landau JM, Huang MT, Newmark HL. Inhibition of carcinogenesis by dietary polyphenolic compounds. *Annu Rev Nutr* 2001;21:381-406.
15. Flora SJS. Structural, chemical and biological aspects of antioxidants for strategies against metal and metalloid exposure. *Oxid Med Cell Longev* 2009;2:191-206.
16. Blois MS. Antioxidant determinations by the use of a stable free radical. *Nature* 1958;18:1199-200.
17. Bujacz A, Zielinski A, Sekula B. Structural studies of bovine, equine, and leporine serum albumin complexes with naproxen. *Proteins* 2014;82:2199-208.
18. Thompson MA. Planaria Software LLC, Seattle, WA, USA. <http://www.arguslab.com>.
19. Jayabharathi J, Thanikachalam V, Venkateshperumal M, Srinivasan N. Fluorescence resonance energy transfer from a bio-active imidazole derivative 2-(1-phenyl-1H-imidazo[4,5-f][1,10]phenanthroline-2-yl)

- phenol to a bioactive indoloquinolizine system. *Spectrochim Acta A* 2011;79:236–44.
20. Sosnowska NS, Siemiarczuk A. A time resolved and steady-state fluorescence quenching study on naproxen and its cyclodextrin complexes in water. *J Photochem Photobiol A* 2001;138:35–40.
 21. Eftink MR, Ghiron CA. Fluorescence quenching studies with proteins. *Anal Biochem* 1981;114:199–227.
 22. Chakraborty B, Basu S. Interaction of BSA with proflavin: a spectroscopic approach. *J Lumin* 2009;129:34–9.
 23. Cao H, Wu D, Wang H, Xu M. Effect of the glycosylation of flavonoids on interaction with protein. *Spectrochim Acta A* 2009;73:972–5.
 24. Gao H, Lei L, Liu J, Qin K, Chen X, Hu Z. The study on the interaction between human serum albumin and a new reagent with antitumour activity by spectrophotometric methods. *J Photochem Photobiol* 2004;167(A):213–21.
 25. Khana SN, Barira Islama YR, Sultana A, Naidu S, Khana AU. Interaction of mitoxantrone with human serum albumin: spectroscopic and molecular modeling studies. *Eur J Pharm Sci* 2008;35:371–82.
 26. Forster T. Intermolecular energy migration and fluorescence. *Ann Phys* 1948;2:55–75.
 27. Jayabharathi J, Jayamoorthy K, Thanikachalam V, Sathishkumar R. Fluorescence quenching of bovine serum albumin by NNMB, fluorescence quenching of bovine serum albumin by NNMB. *Spectrochim Acta Mol Biomol Spectrosc* 2013;108:146–50.
 28. Louis-Jeune C, Andrade-Navarro MA, Perez-Iratxeta C. Prediction of protein secondary structure from circular dichroism using theoretically derived spectra. *Proteins* 2012;80:374–381.
 29. He Y, Wang Y, Tang L, Liu H, Chen W, Zheng Z, et al. Binding of Puerarin to human serum albumin: A spectroscopic analysis and molecular docking. *J Fluoresc* 2008;18:433–42.
 30. Shin WS, Yamashita H, Hirose M. Multiple effects of haemin binding on protease susceptibility of bovine serum albumin and a novel isolation procedure for its large fragment. *Biochem J* 1994;304:81–6.
 31. Venkatesu P, Lee MJ, Lin H. Osmolyte counteracts urea-induced denaturation of α -chymotrypsin. *J Phys Chem B* 2009;113:5327–38.
 32. Attri P, Venkatesu P, Kaushik N, Choi EH. TMAO and sorbitol attenuate the deleterious action of atmospheric pressure non-thermal jet plasma on α -chymotrypsin. *RSC Adv* 2012;2:7146–55.
 33. Attri P, Kumar N, Park JH, Yadav DK, Choi S, Uhm HS, et al. Influence of reactive species on the modification of biomolecules generated from the soft plasma. *Sci Rep* 2015;5:8221.
 34. Attri P, Choi EH. Influence of Reactive oxygen species on the enzyme stability and activity in the presence of ionic liquids. *PLoS One* 2013;8:e75096.
 35. Govindarajan M, Karabasac M, Periandy S, Tanuja D. Spectroscopic (FT-IR, FT-Raman, UV and NMR) investigation and NLO, HOMO–LUMO, NBO analysis of organic 2,4,5-trichloroaniline. *Spectrochim Acta A Mol Biomol Spectrosc* 2012;97:231–45.
 36. Honório KM, Da Silva ABF. An AM1 study on the electron-donating and electron-accepting character of biomolecules. *Int J Quant Chem* 2003;95:126–32.
 37. Pereira DM, Valentão P, Pereira JA, Andrade PB. Phenolics: from chemistry to biology. *Molecules* 2009;14:2202.
 38. Sies H. Polyphenols and health: update and perspectives. *Arch Biochem Biophys* 2010;501:2–5.
 39. Yang CS, Landau JM, Huang MT, Newmark HL. Inhibition of carcinogenesis by dietary polyphenolic compounds. *An Rev Nutr* 2001;21:381–406.
 40. Borges RS, Queiroz AN, Mendes APS, Araújo SC, França LCS, Franco ECS, et al. Density functional theory (DFT) study of edaravone derivatives as antioxidants. *Int J Mol Sci* 2012;13:7594–606.
 41. He XM, Carter DC. Atomic structure and chemistry of human serum albumin. *Nature* 1992;358:209–15.
 42. Roy AS, Dinda AK, Chaudhury S, Dasgupta S. Binding of antioxidant flavonol morin to the native state of bovine serum albumin: Effects of urea and metal ions on the binding. *J Lumin* 2014;145:741–51.
 43. Kelley DI, Mc Clements DJ. Interactions of bovine serum albumin with ionic surfactants in aqueous solutions. *Food Hydrocolloid* 2003;17:73–85.

Supporting information

Additional supporting information may be found in the online version of this article at the publisher's web site.